Lipid oxidation in oil-in-water emulsions: Iron complexation by buffer ions and transfer on the interface as a possible mechanism

Samar Daoud, Elias Bou-Maroun, Gustav Waschatko, Philippe Cayot

Lipid oxidation in oil-in-water emulsions: Iron complexation by buffer ions and transfer on the interface as a possible mechanism

Samar DAOUD[*1], Elias BOU-MAROUN[1], Gustav WASCHATKO[2]& Philippe CAYOT[1]

[1] Unité mixte "Procédés alimentaires et microbiologiques". Université Bourgogne Franche-Comté, AgroSup Dijon, PAM UMR A 02.102, F-21000 Dijon, France

[2] Cargill R&D Centre Europe BVBA Havenstraat 84. B-1800 Vilvoorde, Belgium

* corresponding author: Samar Daoud, E-mail: samar.daoud@u-bourgogne.fr

Highlights

- Iron complexation by buffer influences its ability to initiate oxidation
- The structure of buffer-iron complexes determines its reaction with oxygen
- The charge of oil-water interface modulates the lipid oxidation kinetic
- Buffer-Iron complex could migrate to the positive oil-water interface

ABSTRACT

Lipid oxidation is the main hurdle for omega-3 fatty acid enrichment in food and beverages. Fat oxidation reduces the quality and safety of supplemented products. A tuna oil-in-water emulsion (20% v/v) was exposed to iron-induced oxidation. Emulsions with changing emulsifiers and buffers were analyzed under different storage conditions (argon purging, pH variation) using Conjugated Dienes and Thiobarbituric acid reactive substances assays. The results showed that free iron ions cannot interact with oxygen. However, buffers (Citrate and phosphate) chelate iron ions (Fe (II)). Depending on the pH value and the type of buffer-Fe (II) complex, its prooxidant activity and spatial distribution are influenced. The complex charge defines the interactions with the oil-water interface, i.e., positively charged interfaces repel positively charged complexes which keeps the prooxidant away. The

mechanistic understanding of this work will help formulators and product developers to choose the right buffer and emulsifier combination for oxidation sensitive emulsions.

Keywords

Lipid oxidation

Oil-in-water emulsion

Iron-oxygen complexes

Iron-counter ions complexes

Buffer

Emulsifier

Interfacial charge

1. Introduction

Omega-3 long-chain polyunsaturated fatty acids (ω-3 LC-PUFAs) are ranked very high in consumer awareness and health perception at all ages (Cargill, 2014). Studies showed their contribution to the development of the infant neural system (EFSA, 2014), reduction of cardiovascular disease (He, 2009), and prevention of Alzheimer (Wang et al., 2018), etc. However, the global ω-3 LC-PUFAs intake level is low to very low in most parts of the world (Stark et al., 2016). The World Health Organization recommends higher consumption of these fatty acids (FAO/WHO, 2008). Fish and other marine foods are a great source of ω-3 LC-PUFAs. Consequently, food enrichment with fish oil is becoming a growing trend e.g. enriched milk (Let et al., 2003), etc.

LC-PUFAs are very prone to oxidation due to their high degree of unsaturation (Frankel, 2015). Oxidation reduces significantly product shelf-life. Lipid oxidation causes loss of nutrients, rancidity, and fishy off-flavors. Color and texture of food and beverages may be strongly impacted and even severe health issues and pathologies can be caused by lipid oxidation products (Albert et al., 2013). Aldehydes like 4-hydroxy-2-nonenal (4-HNE) and

4-hydroxy-2-hexenal (4-HHE) were related to adult respiratory distress syndrome, diabetes, and cancer (Liao et al., 2020; Long & Picklo, 2010).

In most food and beverages ω-3 LC-PUFAs are dispersed in an aqueous phase, producing an oil-in-water emulsion. Oxidation in emulsions is known to be mechanistically more complex than in bulk oil (Laguerre et al., 2017). Trace amounts of the prooxidant ions such as iron, copper, or chrome can hardly be avoided in food production. These ions are introduced via contamination in the raw material, piping, or even is wanted for fortification as an effective and sustainable solution to iron deficiency (Martínez-Navarrete et al., 2002). Several mechanisms were proposed to describe the iron-induced lipid oxidation (Cheng & Li, 2007; Schaich, 1992). The Fenton reaction (reaction of iron (II) ions Fe^{2+} with hydrogen peroxide (H_2O_2)) suggested the hydroxyl radical ($OH^{\bullet}$) as the main inducer of lipid oxidation. A second theory proposed an optimum ratio of Fe^{3+}/Fe^{2+}, at this ratio the lipid oxidation was initiated. These theories failed to explain oxidation in some cases and were rejected by several researchers (Cheng & Li, 2007; Qian & Buettner, 1999; Yin et al., 1992). For instance, a linoleic acid emulsion with Fenton reagents could stay stable for hours when the system was separated from ambient air. Besides, when an optimum ratio (1:1) of Fe^{3+}/Fe^{2+} was applied in the same system, the oxidation rate was slower (Yin et al., 1992).

The impact of pH, emulsifier, particle charge and other parameters, on lipid oxidation, were studied separately or combined (Cho et al., 2003; Engelmann, 2003; Fukuzawa et al., 1988; Fukuzawa & Fujii, 1992; Mei et al., 1998; Schaich, 1992; Sørensen et al., 2008). However, the results were inconclusive. In these studies, buffers were added to emulsions (studies on lipid oxidation) or food formulations. Some authors have taken into account the metal-buffer interactions (Engelmann, 2003). Nevertheless, the majority does not indicate the buffer influence. It may result from an underestimation of the possible buffer metal

complexation, or non-availability of complex stability constants in the literature (Ferreira et al., 2015).

Citric acid is one of the most added buffers to food and beverages. It is recognized as an effective flavor enhancer. The understanding of iron-buffer interactions could help researchers and food technologists producing more chemically and physically stable emulsions. This study seeks more insights into the buffer impact on the iron prooxidant potential on lipid oxidation. Tuna oil-in-water emulsion (20% v/v oil) was chosen as a model system. Tuna oil and emulsions were characterized. Various conditions were applied. Several buffers and emulsifiers were tested. The pH level was changed. Oxidation level was measured by conjugated dienes (CD) value and thiobarbituric reactive species (TBArs) value.

2. Materials and methods

Refined tuna oil was produced and supplied by ZOR (A Cargill Company, Zaandam, The Netherlands). Oil was protected by the addition of tocopherols during production. It was purged with Nitrogen and placed in amber glass bottles at -18 °C. The list of reagents and solvents used, is provided in the supplementary data (A).

2.1. Characterization of tuna oil

2.1.1. Fatty acids (FA) composition

Fatty acids composition was measured according to AOAC Method 996.06 with minor modifications (Suseno et al., 2014). Extraction and measurement were repeated three times. First, oil samples (0.18 g), Glyceryl triundecanoate (CAS Number 13552-80-2) as internal standard (0.02 g) (10% w/v), sodium hydroxide solution (0.5 M, 4 mL), isooctane (2 mL) and few boiling chips were placed in a round bottom flask. A water-cooled condenser was attached. Then, the mixture was heated under reflux for 15 min. Boron trifluoride (5 mL) and isooctane (8 mL) were added separately and heated for 5 and 1 min, respectively. Afterward,

97 the flask was left to cool for 15 min. Saturated sodium chloride solution (3 mL) was added. A
98 small scoop of sodium sulfate was placed in a glass tube, and an aliquot of the isooctane layer
99 was added.
100 The standard solution of FAs methyl esters (FAME) was diluted 100 times, and 10 µL
101 of internal standard was added. Analyses were performed using a gas chromatograph (HP
102 6890 series, Germany) equipped with a split/split-less injector (T= 250 °C), a DB-5MS
103 column (30m, i.d. 0.320mm, 0.5 µm film thickness) and mass spectrometer detector
104 5973(MS) (T=250 °C) (Agilent, USA). The carrier gas was Helium (a column flow of
105 1.4 mL/min) and the split ratio was 100:1. The oven temperature program was as follows:
106 11 min at 170 °C, from 170 to 200 °C at 8 °C/min (hold 1.5 min), from 200 to 210 °C at
107 8 °C/min (hold 16 min at 210 °C), from 210 to 300 °C at 20 °C/min (hold 2 min). Finally,
108 fatty acid percentages were determined by internal standardization without taking into account
109 mass response factors. Calculations were performed with the integrated areas, taking into
110 account the internal standard (Equations 1 and 2).

111 $$m\,(FA)(g) = \frac{\text{Area (FA)} * \text{ m (S)}}{\text{Area (S)}} (1)$$

112 $$\%\,(FA) = \frac{\text{m (FA)} * 100}{m_{oil}\,(\text{g})} (2)$$

113 with FA: Fatty acid and S: internal standard. The results were expressed as % of
114 fatty acid/g (oil) (w%/w).

115 *2.1.2. Tocopherol content*

116 The method reported by Gliszczyńska-Świgło & Sikorska, 2004, was used. Oil samples
117 (0.05–0.10 g) were dissolved in 2-propanol (1 mL). Samples were filtered (0.45 µm filter) and
118 transferred to 1 mL vials. Likewise, stock (100 ppm) and working solutions of tocopherols
119 were prepared in 2-propanol. Care was taken to exclude air and light exposure for samples
120 and standard solutions throughout the analytical procedure.

121 Analysis was performed on Shimadzu high-performance liquid chromatography (LC–
122 20AT, Canby, OR, USA) equipped with a C18 Restek column (150mm × 4.6 mm, 5 µm). The
123 UV-visible detector was set at 290 nm. The mobile phase was 50/50 % of
124 acetonitrile/methanol (flow rate of 1 mL/min). The injection volume was 20 µL. Each
125 analysis took 15 min. The α-Tocopherol peak was identified by comparing its retention time
126 to a reference standard (retention time was 7.48 min). The concentration of α-tocopherol was
127 estimated using an external calibration curve (0.5 to 100 ppm and $r^2 = 0.997$) and expressed in
128 $mg.Kg^{-1}$ of oil.

129 *2.1.3. Iron content*

130 Iron concentration in tuna oil was measured using the same method as Liu et al., 2019.
131 Dry ashing method was used to destroy the organic matter. To begin, aliquots (5 g) of tuna oil
132 were heated for more than 8 hours at 102 °C. Next, samples were transferred to the muffle
133 furnace (500 °C) and kept for 10 hours.

134 Thereafter, each sample was dissolved in 25 mL of 2% w/w hydrochloric acid (HCl)
135 solution. Small volumes of HCl solution were added each time and filtered (filter paper). An
136 atomic absorption spectrometer (SpectrAA 220, Varian, Australia) was used with an
137 air/acetylene flame. An iron lamp was set (5 mA, linearity range: 0.06 -15 ppm and
138 248.3 nm). Furthermore, a standard curve was prepared by analyzing solutions containing
139 known iron concentrations (0.05-1 ppm and $r^2 = 0.996$). Each measurement represented an
140 average of three acquisitions and iron content was expressed as $mg.Kg^{-1}$ of oil.

141 *2.2. Emulsion preparation and oxidation conditions*

142 Emulsions were prepared using the same process as our previous study (Daoud et al.,
143 2019) with some slight modifications. Briefly, all emulsions were at 20% (v/v) tuna oil. The
144 aqueous phase was buffer (70% v/v) and (10%v/v) Ferrous (II) sulfate heptahydrate
145 (Fe (II) $SO_4.7\ H_2O$) solutions. Citrate and phosphate were used as buffers (details in

146 supplementary data A). Buffers were prepared at 1 mM concentration, and pH was adjusted
147 using hydrochloric acid (HCl) or sodium hydroxide (NaOH) solutions. Iron solution (1 mM)
148 was added to the aqueous phase (final concentration in emulsions 0.1 mM). Subsequently,
149 emulsifiers at the concentration of 1% (w/v) for Hexadecyltrimethylammonium bromide
150 (CTAB) and sodium dodecyl sulfate (SDS), and 3.7% (w/v) for Tween20 were used to
151 produce the emulsions. Tuna oil and aqueous phase were blended three times (1 min each
152 time) at 20,500 rpm using a rotor/stator homogenizer (Ultra Turrax® T25; IKA-Labortechnik,
153 Munich, Germany). The coarse emulsion was then homogenized four times at 35 MPa using a
154 microfluidizer (LM10; Microfluidics, Westwood, MA, USA).

155 Finally, each preparation was distributed into three vials: 10 mL of each sample were
156 placed in 30 mL vial. In contrast, for the experiment with argon purging, smaller vials (2 mL)
157 were used. The empty vials were purged for 20 seconds prior to the addition of samples.
158 After, emulsions (1 mL) were placed inside and purged for 40 seconds with 5 mL/min flux.
159 These conditions were set to ensure total removal of oxygen dissolved in the emulsion and
160 present in the headspace. Samples were kept in dark at 30°C for 30 days.

161 *2.3. Characterization of oil in water emulsion*

162 *2.3.1. Particle size*

163 The oil droplet size was measured by a Mastersizer 2000 (Malvern Instruments Co.,
164 Ltd., Worcestershire, UK). The emulsion was dispersed in the corresponding buffer to fit the
165 obscuration range (0-12%). The refractive indexes of oil and dispersant (water) were set
166 at 1.48 and 1.33, respectively. The mean of five scans was calculated for each measurement.
167 Moreover, measurements were repeated on three replicates. Data were then analyzed by
168 Mastersizer 3000 software. The particle size distribution was determined by the application of
169 the Mie theory. Then, the volume-surface average diameter ($d_{3,2}$) and volume average

diameter ($d_{4.3}$) were expressed in µm as the mean values of three replicates ± standard deviation.

2.3.2. Particle charge

The oil droplet charge was evaluated by measuring the zeta-potential (mV). A zetameter CAD Zetacompact® (CAD Instrument, Les Essarts Le Roi, France) was used to measure these two parameters. To start, emulsions were greatly diluted in the corresponding buffer solution until a sparser particle distribution. The measurements were carried out at room temperature. Data were presented as an average of three repetitions (separate injections).

2.4. Iron-buffer interaction by UV spectroscopy

Solutions of iron at 0.1 mM and buffers (citrate and phosphate) at 1 mM were prepared. These concentrations were selected to mimic those of prepared emulsions. The UV spectra of these solutions as well as solutions of iron and buffers separately were recorded. Also, solutions of citrate buffer and iron were prepared at different pH values (2.5, 3.9, 5.6, and 7.2). Each sample was measured using a UV-Vis spectrophotometer (UVmc ®, SAFAS, Monaco) with a data interval of 1 nm and a band path of 2 nm. Spectra were recorded in the range of 200 to 800 nm.

2.5. Evaluation of the oxidation level

2.5.1. Determination of the CD value

Before analysis, the fat part was extracted (Daoud et al., 2019). Mixture of isooctane/2-propanol (3:1) (1 mL) and sodium chloride (0.024 g) were added to 0.2 mL of emulsion. The mixture was vortexed for 1 min and left to stand for 1 min for phase separation. Afterward, the upper layer (20-50 µL) was diluted in isooctane. Absorbance spectra were recorded between 200 and 300 nm using a UV-VIS spectrophotometer (UVmc ®, SAFAS, Monaco) with a data interval of 1 nm and a band path of 2 nm. Pure isooctane was used as a

194 reference. The value of CDs was expressed in millimoles of equivalents peroxide per
195 kilogram of oil (mmol eq peroxide·kg^{-1}_{oil}) using a molar extinction coefficient of
196 27000 M^{-1}·cm^{-1} at 233 nm.

197 *2.5.2. Determination of TBArs value*

198 TBArs value was determined according to the original method described by (Mcdonald
199 & Hultin, 1987). Briefly, TBA reagent was prepared by mixing 0.375 g of thiobarbituric acid
200 (TBA), 15 g of trichloroacetic acid (TCA), 1.76 mL of HCl, and 98.24 mL of water. To avoid
201 further oxidation, 3 mL of a 2% solution of Butylated hydroxytoluene (BHT) in Ethanol was
202 added to 100 mL of TBA reagent. Then, 100 µL of emulsion, 400 µL of water, and 1 mL of
203 TBA reagent were mixed in Eppendorf tube (2 mL capacity). Samples were placed in a water
204 bath (100 °C for 15 min). Samples were left to cool down for 3 min before centrifuging
205 for1 min at 10000 rpm using Eppendorf® Microcentrifuge 5415D (Eppendorf AG,
206 Barkhausenweg, Hamburg, Germany). Once the upper layer was transferred directly or
207 diluted to the cuvette, the UV-spectra were recorded in the range of 500 to 600 nm using the
208 UV-Vis spectrophotometer (UVmc ®, SAFAS, Monaco). The data interval was set at 1 nm
209 and the band path at 2 nm. The concentration of aldehydes was calculated using the standard
210 curve. The standard curve was prepared with tetramethoxypropane (TMP): eight standards,
211 ranging from 0 to 30 µM and r^2 = 0.999. TBArs value was expressed in millimolars of
212 equivalents malondialdehyde per liter of emulsion (mM eq MDA.L^{-1} of emulsion).

213 *2.6. Statistical tests*

214 To assess significant differences, analysis of variance (one-way ANOVA) followed by
215 means comparison using the Tukey test was applied. The level of significance was set to 95%
216 (p= 0.05). Statistical tests were performed using the Minitab® (version 18.1; PA, USA).

3. Results and discussion

3.1. Preliminary test: defining the major parameters of lipid oxidation

Emulsion with 1 mM citrate buffer at pH 7 and iron solution (0.1 mM) was prepared and placed in 2 mL vials (ratio emulsion to the headspace of 1 (v/v)). The oxidation level was evaluated by CD values. A lag phase of 5 days was noticed (Figure 1). CD value increased after attaining a maximum of 112 mmol eq peroxide.Kg^{-1}_{oil} and then decreased. This phenomenon is frequently observed with CD or peroxide value records. The primary product content increases with the degree of oxidation and reaches a maximum. Afterward, the primary products (peroxides) are transformed in secondary products which results in a decrease in their concentration.

Fish oil was used in this study because of its low oxidative stability. Its FA composition confirmed it (Table 1). The repartition of fatty acids was in good compliance with the codex of fish oils (Codex Alimentarius Commission, FAO, WHO, 2017), and other researchers' works (Nazir et al., 2017; Suseno et al., 2014). In general, the tuna oil was dominated by palmitic acid (C 16:0) (19.5 %wt.) as the major saturated fatty acids (SFAs) and oleic acid (C18:1) (18.8 %wt.) as the main monounsaturated fatty acids (MUFAs). As for polyunsaturated fatty acids (PUFAs), eicosapentaenoic acid (EPA) (8.9 %wt.) and docosahexaenoic acid (DHA) (25.3 %wt.) were the most abundant. The total PUFAs in tuna oil reached 41.2 %wt. It is well known that the ability to be oxidized could be linearly related to the number of bis-allylic positions present in the fatty esters (two times higher for every active bis-allylic methylene group) (Frankel, 2015). In addition, the decomposition of hydroperoxides starts earlier in the presence of a high amount of PUFA, which confirms the rapid drop of the CD values (Figure 1a). Besides, the initial iron content in tuna oil was estimated as 0.71 ± 0.35 $mg.Kg^{-1}$ of oil (Table 1). Iron content in fish oil should be within the range of 0.5 to 7 $mg.Kg^{-1}$ for crude oil and ≤ 1.5 $mg.Kg^{-1}$ for refined fish oil (Hoan & Son,

2018). However, the lag phase was seen because tuna oil was enriched with tocopherol (vitamin E). The α-Tocopherol content in oil used in this study was about 1282 $mg.Kg^{-1}{}_{oil}$ (Table 1). A maximum amount of 6000 $mg.Kg^{-1}$ of α-Tocopherol or mixture can be added to preserve fish oil (Codex Alimentarius Commission, FAO, WHO, 2017). α-Tocopherol (AH) reacts rapidly with peroxyl radicals ($LOO^{\cdot}$)(Equation 3). This reaction is faster than the reaction of peroxyl radicals with other lipid molecules (LH) (Equation 4).

$$LOO^{\cdot} + AH \rightarrow LOOH + A^{\cdot} \quad (10^{6} M^{-1} S^{-1}) \quad (3)$$

$$LOO^{\cdot} + LH \rightarrow LOOH + L^{\cdot} \quad (10^{1} M^{-1} S^{-1}) \quad (4)$$

By hydrogen atom donation, lipid hydroperoxides (LOOH) and tocopherol radical ($A^{\cdot}$) are produced. Tocopherol radical is stable by resonance thus, the radical chain reaction does not propagate (Frankel, 2015).

Afterward, the same experiment was repeated but emulsion was purged with argon. Flushing emulsion with argon provided an inert atmosphere. Hence, conjugated dienes values of these samples remained permanently low during several weeks (Figure 1). Regardless of some fluctuations, no significant changes were observed over the storage period (one-way ANOVA $p<0.05$) (supplementary data (B)). Identical results were obtained for emulsions with phosphate buffer (10 mM) and iron (0.01 mM). Nitrogen and argon-purged emulsions remained stable over 30 days of storage (supplementary data (B)). The unique presence of iron is insufficient for initiating lipid radicalization. Consequently, complete hypoxia is a great way to preserve fragile oil against oxidation (Yin et al., 1992).

A positively charged emulsifier (CTAB) was used with the preconception that positively charged ferric ions cannot reach a positively charged interface. However, the iron ions (Fe^{2+} / Fe^{3+}), in the presence of oxygen, were able to reach the interface. Hypervalent iron-oxygen complexes such as ferryl (IV) $(FeO)^{2+}$, perferryl (V) $(FeO)^{3+}$, or mixed iron oxygen complexes (Fe^{2+}-O_2-Fe^{3+}) were mentioned as responsible for lipid oxidation (Cheng

& Li, 2007; Lee et al., 2010; Qian & Buettner, 1999; Schaich, 1992). These species have a high redox potential and are stereospecific oxidants in H-abstraction. The dioxygen (triplet state) cannot react directly with iron (singlet state), because of spin restriction. Nevertheless, iron chelation induces a significant energy rearrangement to "3d" or "4s" orbitals, resulting in the removal of the spin barrier (Yin et al., 1992). In this experiment, chelators were not added. Some authors mentioned the potential of buffers (phosphate, citrate…) to compete with iron chelators (Ferreira et al., 2015; Yin et al., 1992). Could buffers chelate iron and help its interaction with oxygen? What is the reactivity of buffer-iron-oxygen complexes?

3.2. Buffer role in lipid oxidation

A new set of samples was prepared with iron solution at 0.1 mM. Two buffers were tested: citrate and phosphate. The pH was set at 7 (buffer at 1 mM). The oxidation level was monitored using the CD value.

CD values increased rapidly from approx. 50 to 250 mmol eq peroxide.Kg^{-1}_{oil} (Figure 2a). It was noticed that the buffer type impacted on lipid oxidation. Only after three days, the CD values of these two emulsions were significantly different (one-way ANOVA based on buffer's type; $p<0.05$). Moreover, the induction time was determined by the time when the CD value was significantly different than the day before (one-way ANOVA with the time factor, supplementary data (C)). Induction times were between seven to ten days for citrate and four days for phosphate (designated by arrows in Figure 2a). Thus, the emulsion with citrate buffer was the most stable.

Besides, iron complexation by buffers changes according to the pKa and pH values (Kristinova et al., 2014). As shown in Figure 2b, citric acid has three values of pKa (3.13, 4.76, and 6.4) and phosphate has also three (2.15, 7.2, and 12.33). At pH 7, the citrate (Cit^{3-}) is in majority in comparison of monohydrogenocitrate:

$$pH = pKa + \log\frac{Base}{acid} = pKa + \log\frac{[Cit^{3-}]}{[CitH^{2-}]} \quad (5)$$

$$\frac{[Cit^{3-}]}{[CitH^{2-}]} = 10^{(pH-pKa)} = 10^{(7-6.4)} = 3.98 \quad (6)$$

The percentage of Cit^{3-} of the total citrate (Cit^{3-} + $CitH^{2-}$) can be estimated as follow:

$$\frac{[Cit^{3-}]}{[Cit^{3-}] + [CitH^{2-}]} = \frac{3.98\,[CitH^{2-}]}{3.98\,[CitH^{2-}] + [CitH^{2-}]} = \frac{3.98}{1 + 3.98} = 0.799 \quad (7)$$

The totality of citric acid is charged: approximately 80% is totally deprotonated (Cit^{3-}) and the rest is monohydrogenocitrate ($CitH^{2-}$). Following the same strategy (Equations 5, 6, and 7), the distribution of phosphate species can be defined. At pH 7, phosphate is mainly presented as dihydrogenophosphate $H_2PO_4^-$ (61%), and monohydrogenophosphate HPO_4^{2-} (39%). All of these species are negatively charged and can play the role of counter-ion (iron ions or hypervalent iron-oxygen complexes).

Citrate and phosphate can complex iron (Cho et al., 2003; Ferreira et al., 2015; Yin et al., 1992). These complexes can be detected at 250 and 275 nm after the addition of iron to citrate and phosphate solutions, respectively (supplementary data (C)). The peaks were also mentioned in other studies (Francis & Dodge, 1993; Königsberger et al., 2000; Seraghni et al., 2012; Yin et al., 1992).

The complexation of ferrous ions with citrate and phosphate buffers as the constants of complexation (logβ) is presented in reactions (8 and 9) and (10 and 11), respectively (Königsberger et al., 2000; Mao et al., 2011).

$$Fe^{2+} + HCit^{2-} \rightarrow FeHCit \ (\log\beta = \frac{[FeHCit]}{[Fe^{2+}][HCit^{2-}]} = 10.17) \quad (8)$$

$$Fe^{2+} + Cit^{3-} \rightarrow FeCit^{-} \ (\log\beta = \frac{[FeCit^{-}]}{[Fe^{2+}][Cit^{3-}]} = 6.13) \quad (9)$$

$$Fe^{2+} + H_2PO_4^{-} \rightarrow FeH_2PO_4^{+} \ (\log\beta = \frac{[FeH_2PO_4^{+}]}{[Fe^{2+}][H_2PO_4^{-}]} = 22.3) \quad (10)$$

312 $$Fe^{2+} + HPO_4^{2-} \rightarrow FeHPO_4 \ (\log\beta = \frac{[FeHPO_4]}{[Fe^{2+}][HPO_4^{2-}]} = 16) \ (11)$$

313 Phosphate buffer had higher values of stability constants ($\log\beta$). The resulting
314 complexes are mainly positively charged ($FeH_2PO_4^+$) (reactions 10 and 11). In contrast, the
315 majority of iron (II) -citrate complex is negatively charged ($FeCit^-$). Can iron complexation by
316 buffer impact its position in the emulsion? Can iron-citrate complex migrate towards the
317 positively charged interface?

318 *3.3. Impact of buffer on iron location and activity in the emulsion*

319 Emulsions were prepared with citrate buffer (1 mM), CTAB as an emulsifier, and
320 iron (II) solution at 0.1 mM. Four pH levels were tested: 2.5, 3.9, 5.6, and 7.2. All samples
321 were kept in dark at 30 °C.

322 First, the particle size was measured. The values of $d_{3:2}$ ranged from 0.53 to 0.57 µm and
323 $d_{4:3}$ from 0.56 to 0.62 µm. At pH 7.2, droplets were slightly bigger. But no significant changes
324 were seen regarding the pH (one-way ANOVA analysis $p<0.05$, applied on $d_{4:3}$ and $d_{3:2}$
325 values) (details in supplementary data (D)). All emulsions were stable: no coalescence or
326 flocculation was observed over the storage period. The particle charge was evaluated by the
327 variations of mobility (µm/s/V/cm) and zeta-potential (mV) (supplementary data (D)). CTAB
328 is always positively charged: it is permanent quaternary ammonium ($R_1R_2R_3R_4N^+$) and the pH
329 does not influence its charge (no proton exchange). However, when the pH of emulsions
330 increased, the zeta-potential decreased from 43 to 14 mV, then flipped to negative values of --
331 15 and -30 mV (Figure 3a). At different pH, several species of citrate are present in the
332 solutions (Figure 3a). For instance, at pH 2.5 citrate is mainly protonated (81% of acid, H_3Cit,
333 and 19% of the conjugated base H_2Cit^-). Complexation of iron by citrate is low. Citrate cannot
334 transfer irons ions, the interface charge remained positive. When the pH increase, citrate is
335 gradually deprotonated. It is more available to complex iron ions and conveys it to the

interface. Iron-Citrate complex changes the apparent charge at the interface. In general, the zeta-potential is a great representation of the electrical characteristics of an emulsion droplet because it inherently accounts for the adsorption of any charged counter-ions (Cano-Sarmiento et al., 2018). The charge of iron-citrate complexes varies from positive to more negative with increasing pH. This phenomenon was also mentioned in other studies (Fukuzawa, 2008).

At a higher level of pH, iron complexation by citrate becomes more important. It was proved by the UV-spectra of the iron-citrate solutions (at different pH) (Figure 3b). The spectra of iron and citrate solutions alone were reduced from the solutions spectra. When the pH increase, the peak of the iron-citrate complex near 250 nm increased. Citrate comprised more possible sites to complex iron. The resulting complex migrates to the interface and amends its absolute charge. The state of emulsion interface and the possible migration of iron-oxygen-buffer complexes are schematized in Figure 3a.

Iron complexation by citrate facilitates its migration near the interface (CTAB as an emulsifier). However, when citrate was used as a buffer the emulsion was more stable to oxidation. Complexation affinity cannot explain alone the difference in the oxidation levels of the two prepared emulsions. When iron complexation was considered retarding lipid oxidation, in several cases, it was the opposite. For instance, the stability constants of diethylenetriaminepentaacetic acid (DTPA) and ethylenediaminetetraacetic acid (EDTA) with iron (II) ions are very similar. Their addition led to different oxidation rates in iron (II)-linoleic acid emulsion (Yin et al., 1992). The reaction of complexed-Fe (II) with oxygen is mainly controlled by the structure of this complex. To be able to react with oxygen, complexed-iron should still present at least one free site or occupied by a labile water molecule. When reaction with oxygen is possible, the Fe (II) autoxidation can occur

360 (production of Fe (III) -complex), Fe (II) -complex-O_2 is no more present to accelerate lipid
361 oxidation.

362 In the presence of citrate, nuclear magnetic studies confirmed that the ferrous citrate
363 complex ($FeCit^-$) is tridentate. Fe (II) is involved with two carboxylic acid groups and the
364 hydroxyl group of citrate and the fourth bond is with a water molecule (Francis & Dodge,
365 1993). This structure eases the autoxidation of the ferrous citrate complex. This fast
366 autoxidation retards the initiation of lipid oxidation. Other studies conferred about the
367 presence of a dimeric iron citrate complex ($FeCit_2^{4-}$) at pH 7 ($\log\beta = 7$). The formation of this
368 dimeric complex also increased the iron (II) oxidation rate: in the presence of citrate (ratio of
369 1:10 (iron: citrate)) oxidation rate was at least two times higher (Pham & Waite, 2008).
370 A speciation study on Fe (II) autoxidation kinetics in the presence of phosphate, showed
371 that $FeH_2PO_4^+$ and $FeHPO_4$ are the two major phosphates complexes at pH 6.5-7.5 (Mao et
372 al., 2011). Both complexes do not promote iron autoxidation. As a result, these phosphate-
373 iron complexes are more available to initiate lipid oxidation. These findings comply with the
374 oxidative stability seen higher for emulsion with citrate buffer compared to phosphate buffer.
375 Since the structure and charge of resulting complexes are important, the interface charge has
376 also a role in lipid oxidation.

377 *3.4. Impact of interface charge on lipid oxidation*

378 Three emulsions were prepared at both pH 2.5 and 7.2. The same buffer and iron
379 concentrations were maintained. Three emulsifiers were tested: CTAB (positively charged),
380 Tween20 (no charge), and SDS (negatively charged).
381 The particle size of emulsions with SDS and Tween20 were in the same range of
382 emulsions with CTAB emulsifier. Emulsions stabilized with SDS had $d_{4:3}$ of
383 0.569 ± 0.008 µm and $d_{3:2}$ of 0.538 ± 0.006 µm. Emulsions with Tween20 emulsifier also
384 presented lower values of $d_{4:3}$ (0.528 ± 0.001 µm) and $d_{3:2}$ (0.5 ± 0.001 µm). The zeta

potential values were 7.69 ± 1 and 3.09 ± 7.2 mV respectively for SDS and Tween20 stabilized emulsions. The zeta potential of the emulsions prepared with Tween 20 and SDS was less important compared to emulsion prepared with CTAB emulsifier.

At pH 2.5, there was no significant difference in the CD values (test of equal variance $p<0.05$) (supplementary data (E)). In contrast, the TBArs test presented some significant variations (Figure 4a). At pH 2.5, emulsions with CTAB emulsifier revealed no changes in TBArs values through the storage time (test for equal variance $p<0.05$). The TBArs of emulsion with SDS was significantly increasing since the first day. A similar phenomenon was identified for emulsion with a neutral interface (Tween20) but with a lower extent.

At pH 7.2, the citrate (86% Cit^{3-}) is in majority in comparison of monohydrogenocitrate (14 % $CitH^{2-}$) (ions distribution obtained by equations 5, 6 and 7, with pH = 7.2 and pKa = 6.4). The neutral Tween20 emulsifier presented the most stable emulsion (slight variations seen with one-way ANOVA $p<0.05$). The CD values were lower than those with CTAB and SDS emulsifiers. Once again SDS emulsion was the less stable (supplementary data (E)). As for TBArs values, the same order as at pH 2.5 was noticed, SDS stabilized emulsion was the less stable emulsion followed by Tween20 and CTAB emulsion (Figure 4b).

Compared to SDS and Tween20, CTAB-emulsion was more stable. TBArs values at pH 2.5 and 7.2 were almost stable during the storage time (Figure 4). The positively charged interface repelled iron ions and retarded the oxidation. SDS negatively charged interface attracted iron and iron-oxygen ions. Hence, iron was closer to the peroxides molecules (LOOH) (present near the interface due to their hydrophilic head). Iron ions decomposed peroxides to form alkoxyl ($LO^{\bullet}$) radicals (Equation 12). These interactions accelerated the lipid oxidation rate.

$$Fe^{2+} + LOOH \rightarrow LO^{\cdot} + Fe^{3+} + OH^{-} \quad (12)$$

For instance, at pH 2.5, the initial TBArs value of SDS-emulsion was 12 and 26 times higher than Tween20 and CTAB emulsions. As for Tween20 emulsion, iron ions could still approach the interface through ion-dipole interactions. However, these interactions are weaker than ion-ion interactions (Mei et al., 1998; Schaich, 1992).

Moreover, the important oxidation in negatively charged emulsion could be associated with the rapid tocopherol oxidation in such emulsion. Iron ions (attracted by the interface) can interact with tocopherol molecules (binding to SO_3^- group of SDS by hydrogen bond). Tocopherol (AH) can regenerate Fe^{3+} into Fe^{2+} (Equation 13). Ferrous ions are then available to induce more oxidation near the interface.

$$AH + Fe^{3+} \rightarrow A^{\cdot} + Fe^{2+} + H^{+} \quad (13)$$

Iron complexation and transfer far from the interface can inhibit lipid oxidation. However, in the case, complexed iron (II) was near the interface. With a positively charged interface, tocopherol is more preserved and can react as a radical scavenger (Fukuzawa et al., 1988; Kristinova et al., 2014).

CD and TBArs values followed the same trend at pH 2.5 and 7.2. The oxidative stability can be ranked in descending order: CTAB > Tween20 > SDS. However, at pH 2.5, the CD and TBArs values were generally higher than those at pH 7.2. For instance, the CD and TBArs values of emulsion with SDS emulsifier were respectively 3 and 10 times higher at acidic pH. As for Tween20 emulsions, the TBArs values present lag phases at pH 7.2 (Figure 4b), in contrast, it increased immediately at pH 2.5 (Figure 4a). Similar trends were seen for CTAB emulsions: TBArs values were approx. two times higher at lower pH value. At pH 2.5, citrate was mostly protonated (81% $CitH_3$), which lead to low iron complexation (Figure 3). Thus, iron could be mainly present as free ions. Iron can then rapidly migrate to the oil-water interface and increase the oxidation level. When the interface is negatively charged (SDS emulsifier) the phenomena are more important. At higher pH, citrate ($HCit^2$ &

434 Cit^{3}) can complex iron, and by this performs a protective role, oxidation is less important.
435 However, iron is not fully complexed, and therefore oxidation is not totally stopped. Identical
436 results were obtained for corn oil-in-water emulsion (Cho et al., 2003).

437 **4. Conclusion**

438 Iron (endogenous or exogenous) can significantly accelerate the lipid oxidation in
439 oil-in-water emulsions. The iron-oxygen interactions constitute the first step of lipid
440 oxidation. Hence, an absolute reduction of oxygen could limit lipid oxidation even with iron
441 presence. Such a solution is not practical nor economical for food industries. Conversely, the
442 buffer and emulsifier choice can control the oxidation-initiation in emulsions. Buffers chelate
443 iron ions, and in this way impact its position and prooxidant potential. Factors like pH
444 (protonation of chelator; pKa values), chelator's affinity to Fe (II) (Binding constants; $\log\beta$),
445 and the final structure of the complex (number of free coordination sites) influence its
446 stability and catalytic activity. When the complex structure promotes the iron-autoxidation,
447 oxidation initiation by this complex is retarded. In addition, the buffer-iron complexes allow
448 iron migration near the positively charged interface, overcoming the repulsive forces.
449 Therefore, the interface charge has a critical impact on lipid oxidation. Negatively charged
450 interface increases the rate of oxidation by attracting free and chelated irons ions. Besides,
451 α-tocopherol near this interface is closer to iron ions which promote its oxidation and Fe (II)
452 regeneration. Consequently, controlling iron ions interactions with buffers and emulsifiers
453 could help to limit omega-3 LC-PUFA oxidation in food and drinks.

454 **Acknowledgements**

455 The authors gratefully acknowledge our partner Cargill, the "Fonds Européen de
456 Developpement Régional" (FEDER), and the Regional Council of Bourgogne-Franche-

Comté, for their financial support. The authors would like thinking all people who helped in the experimental work, especially Miss Hoang Phuong Ha.

Conflict of interest

The authors declare that there is no conflict of interest.

References

Albert, B. B., Cameron-Smith, D., Hofman, P. L., & Cutfield, W. S. (2013). Oxidation of Marine Omega-3 Supplements and Human Health. *BioMed Research International*, *2013*, 1–8. https://doi.org/10.1155/2013/464921

Cano-Sarmiento, C., Téllez-Medina, D. I., Viveros-Contreras, R., Cornejo-Mazón, M., Figueroa-Hernández, C. Y., García-Armenta, E., Alamilla-Beltrán, L., García, H. S., & Gutiérrez-López, G. F. (2018). Zeta Potential of Food Matrices. *Food Engineering Reviews*, *10*(3), 113–138. https://doi.org/10.1007/s12393-018-9176-z

Cargill. (2014). *Study shows consumers want more omega-3 | Cargill*. https://www.cargill.com/news/releases/2014/NA31701258.jsp

Cheng, Z., & Li, Y. (2007). What Is Responsible for the Initiating Chemistry of Iron-Mediated Lipid Peroxidation: An Update. *Chemical Reviews*, *107*(3), 748–766. https://doi.org/10.1021/cr040077w

Cho, Y.-J., Alamed, J., McClements, D. j., & Decker, E. a. (2003). Ability of Chelators to Alter the Physical Location and Prooxidant Activity of Iron in Oil-in-Water Emulsions. *Journal of Food Science*, *68*(6), 1952–1957. https://doi.org/10.1111/j.1365-2621.2003.tb07000.x

Codex Alimentarius Commission, FAO, WHO. (2017, Adopted in). *Standard for fish oils, CXS 329-2017*. http://www.fao.org/fao-who-codexalimentarius

Daoud, S., Bou-maroun, E., Dujourdy, L., Waschatko, G., Billecke, N., & Cayot, P. (2019). Fast and direct analysis of oxidation levels of oil-in-water emulsions using ATR-

FTIR. *Food Chemistry*, *293*, 307–314. https://doi.org/10.1016/j.foodchem.2019.05.005

EFSA. (2014). Scientific Opinion on the substantiation of a health claim related to DHA and contribution to normal brain development pursuant to Article 14 of Regulation (EC) No 1924/2006. *EFSA Journal*, *12*(10), 3840. https://doi.org/10.2903/j.efsa.2014.3840

Engelmann, M. D. (2003). Variability of the Fenton reaction characteristics of the EDTA, DTPA, and citrate complexes of iron. *BioMetals*, *16*(4), 519–527. https://doi.org/10.1023/A:1023480617038

FAO/WHO. (2008, November 10). WHO | Joint FAO/WHO Expert Consultation on Fats and Fatty Acids in Human Nutrition (10 - 14 November 2008, WHO, Geneva). *WHO*. https://www.who.int/nutrition/topics/FFA_interim_recommendations/en/

Ferreira, C. M. H., Pinto, I. S. S., Soares, E. V., & Soares, H. M. V. M. (2015). (Un)suitability of the use of pH buffers in biological, biochemical and environmental studies and their interaction with metal ions – a review. *RSC Advances*, *5*(39), 30989–31003. https://doi.org/10.1039/C4RA15453C

Francis, A. J., & Dodge, C. J. (1993). Influence of Complex Structure on the Biodegradation of Iron-Citrate Complexes. *Applied and Environmental Microbiology*, *59*(1), 109–113. https://doi.org/10.1128/AEM.59.1.109-113.1993

Frankel, E. N. (2015). *Lipid Oxidation* (Second edition). Woodhead Publishing.

Fukuzawa, K. (2008). Dynamics of lipid peroxidation and antioxidion of alpha-tocopherol in membranes. *Journal of Nutritional Science and Vitaminology*, *54*(4), 273–285.

Fukuzawa, K., & Fujii, T. (1992). Peroxide dependent and independent lipid peroxidation: Site-specific mechanisms of initiation by chelated iron and inhibition by α-tocopherol. *Lipids*, *27*(3), 227–233. https://doi.org/10.1007/BF02536183

506 Fukuzawa, K., Kishikawa, K., Tadokoro, T., Tokumura, A., Tsukatani, H., & Gebicki, J. M.
507 (1988). The effects of α-tocopherol on site-specific lipid peroxidation induced by iron
508 in charged micelles. *Archives of Biochemistry and Biophysics*, *260*(1), 153–160.
509 https://doi.org/10.1016/0003-9861(88)90436-5
510 Gliszczyńska-Świgło, A., & Sikorska, E. (2004). Simple reversed-phase liquid
511 chromatography method for determination of tocopherols in edible plant oils. *Journal*
512 *of Chromatography A*, *1048*(2), 195–198.
513 https://doi.org/10.1016/j.chroma.2004.07.051
514 He, K. (2009). Fish, Long-Chain Omega-3 Polyunsaturated Fatty Acids and Prevention of
515 Cardiovascular Disease—Eat Fish or Take Fish Oil Supplement? *Progress in*
516 *Cardiovascular Diseases*, *52*(2), 95–114. https://doi.org/10.1016/j.pcad.2009.06.003
517 Hoan, P. T., & Son, T. K. (2018). Tra Catfish Oil Production: Phospholipid Removal Using
518 Citric Acid and Bleaching Using Activated Carbon. *2018 4th International*
519 *Conference on Green Technology and Sustainable Development (GTSD)*, 528–532.
520 https://doi.org/10.1109/GTSD.2018.8595528
521 Königsberger, L.-C., Königsberger, E., May, P. M., & Hefter, G. T. (2000). Complexation of
522 iron(III) and iron(II) by citrate. Implications for iron speciation in blood plasma.
523 *Journal of Inorganic Biochemistry*, *78*(3), 175–184. https://doi.org/10.1016/S0162-
524 0134(99)00222-6
525 Kristinova, V., Aaneby, J., Mozuraityte, R., Storrø, I., & Rustad, T. (2014). The effect of
526 dietary antioxidants on iron-mediated lipid peroxidation in marine emulsions studied
527 by measurement of dissolved oxygen consumption. *European Journal of Lipid Science*
528 *and Technology*, *116*(7), 857–871. https://doi.org/10.1002/ejlt.201400011

Laguerre, M., Bily, A., Roller, M., & Birtić, S. (2017). Mass Transport Phenomena in Lipid Oxidation and Antioxidation. *Annual Review of Food Science and Technology*, *8*(1), 391–411. https://doi.org/10.1146/annurev-food-030216-025812

Lee, Y.-M., Hong, S., Morimoto, Y., Shin, W., Fukuzumi, S., & Nam, W. (2010). Dioxygen Activation by a Non-Heme Iron(II) Complex: Formation of an Iron(IV)−Oxo Complex via C−H Activation by a Putative Iron(III)−Superoxo Species. *Journal of the American Chemical Society*, *132*(31), 10668–10670. https://doi.org/10.1021/ja103903c

Let, M. B., Jacobsen, C., Frankel, E. N., & Meyer, A. S. (2003). Oxidative flavour deterioration of fish oil enriched milk. *European Journal of Lipid Science and Technology*, *105*(9), 518–528. https://doi.org/10.1002/ejlt.200300821

Liao, H., Zhu, M., & Chen, Y. (2020). 4-Hydroxy-2-nonenal in food products: A review of the toxicity, occurrence, mitigation strategies and analysis methods. *Trends in Food Science & Technology*, *96*, 188–198. https://doi.org/10.1016/j.tifs.2019.12.011

Liu, J., Guo, Y., Li, X., Si, T., McClements, D. J., & Ma, C. (2019). Effects of Chelating Agents and Salts on Interfacial Properties and Lipid Oxidation in Oil-in-Water Emulsions. *Journal of Agricultural and Food Chemistry*, acs.jafc.8b05867. https://doi.org/10.1021/acs.jafc.8b05867

Long, E. K., & Picklo, M. J. (2010). Trans-4-hydroxy-2-hexenal, a product of n-3 fatty acid peroxidation: Make some room HNE…. *Free Radical Biology and Medicine*, *49*(1), 1–8. https://doi.org/10.1016/j.freeradbiomed.2010.03.015

Mao, Y., Pham, A. N., Rose, A. L., & Waite, T. D. (2011). Influence of phosphate on the oxidation kinetics of nanomolar Fe(II) in aqueous solution at circumneutral pH. *Geochimica et Cosmochimica Acta*, *75*(16), 4601–4610. https://doi.org/10.1016/j.gca.2011.05.031

554 Martínez-Navarrete, N., Camacho, M. M., Martínez-Lahuerta, J., Martínez-Monzó, J., & Fito,
555 P. (2002). Iron deficiency and iron fortified foods—a review. *Food Research*
556 *International*, *35*(2), 225–231. https://doi.org/10.1016/S0963-9969(01)00189-2
557 Mcdonald, R. E., & Hultin, H. O. (1987). Some Characteristics of the Enzymic Lipid
558 Peroxidation System in the Microsomal Fraction of Flounder Skeletal Muscle. *Journal*
559 *of Food Science*, *52*(1), 15–21. https://doi.org/10.1111/j.1365-2621.1987.tb13964.x
560 Mei, L., McClements, D. J., Wu, J., & Decker, E. A. (1998). Iron-catalyzed lipid oxidation in
561 emulsion as affected by surfactant, pH and NaCl. *Food Chemistry*, *61*(3), 307–312.
562 https://doi.org/10.1016/S0308-8146(97)00058-7
563 Nazir, N., Diana, A., & Sayuti, K. (2017). Physicochemical and Fatty Acid Profile of Fish Oil
564 from Head of Tuna (Thunnus albacares) Extracted from Various Extraction Method.
565 *International Journal on Advanced Science, Engineering and Information Technology*,
566 *7*(2), 709. https://doi.org/10.18517/ijaseit.7.2.2339
567 Pham, A. N., & Waite, T. D. (2008). Oxygenation of Fe(II) in the Presence of Citrate in
568 Aqueous Solutions at pH 6.0−8.0 and 25 °C: Interpretation from an Fe(II)/Citrate
569 Speciation Perspective. *The Journal of Physical Chemistry A*, *112*(4), 643–651.
570 https://doi.org/10.1021/jp077219l
571 Qian, S. Y., & Buettner, G. R. (1999). Iron and dioxygen chemistry is an important route to
572 initiation of biological free radical oxidations: an electron paramagnetic resonance
573 spin trapping study. *Free Radical Biology and Medicine*, *26*(11), 1447–1456.
574 https://doi.org/10.1016/S0891-5849(99)00002-7
575 Schaich, K. M. (1992). Metals and lipid oxidation. Contemporary issues. *Lipids*, *27*(3), 209–
576 218. https://doi.org/10.1007/BF02536181
577 Seraghni, N., Belattar, S., Mameri, Y., Debbache, N., & Sehili, T. (2012). Fe(III)-Citrate-
578 Complex-Induced Photooxidation of 3-Methylphenol in Aqueous Solution.

International Journal of Photoenergy, *2012*, 1–10. https://doi.org/10.1155/2012/630425

Sørensen, A.-D. M., Haahr, A.-M., Becker, E. M., Skibsted, L. H., Bergenståhl, B., Nilsson, L., & Jacobsen, C. (2008). Interactions between Iron, Phenolic Compounds, Emulsifiers, and pH in Omega-3-Enriched Oil-in-Water Emulsions. *Journal of Agricultural and Food Chemistry*, *56*(5), 1740–1750. https://doi.org/10.1021/jf072946z

Stark, K. D., Van Elswyk, M. E., Higgins, M. R., Weatherford, C. A., & Salem, N. (2016). Global survey of the omega-3 fatty acids, docosahexaenoic acid and eicosapentaenoic acid in the blood stream of healthy adults. *Progress in Lipid Research*, *63*, 132–152. https://doi.org/10.1016/j.plipres.2016.05.001

Suseno, S. H., Saraswati, Hayati, S., & Izaki, A. F. (2014). Fatty Acid Composition of Some Potential Fish Oil from Production Centers in Indonesia. *Oriental Journal of Chemistry*, *30*(3), 975–980.

Wang, L., Fan, H., He, J., Wang, L., Tian, Z., & Wang, C. (2018). Protective effects of omega-3 fatty acids against Alzheimer's disease in rat brain endothelial cells. *Brain and Behavior*, *8*(11). https://doi.org/10.1002/brb3.1037

Yin, D., Lingnert, H., Ekstrand, B., & Brunk, U. T. (1992). Fenton reagents may not initiate lipid peroxidation in an emulsified linoleic acid model system. *Free Radical Biology and Medicine*, *13*(5), 543–556. https://doi.org/10.1016/0891-5849(92)90149-B

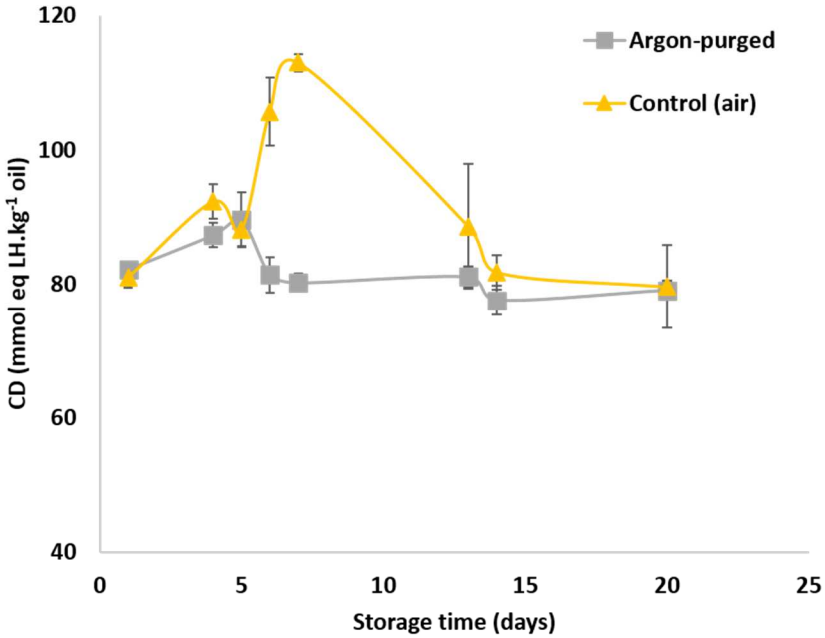

Figure 1. Lipid oxidation as measured by conjugated dienes (CD mmol eq peroxide.Kg^{-1} of oil) for 20% (v/v) tuna oil-in-water emulsions with citrate buffer (1 mM) and iron (II) (0.1 mM). Two conditions were studied: (▲) under control atmosphere, air (dioxygen solubilized in the emulsion) and (■) after purging with argon (hypoxic condition). Samples were kept in dark at 30 °C. Data are means of three repetitions. Error bars represent standard deviations

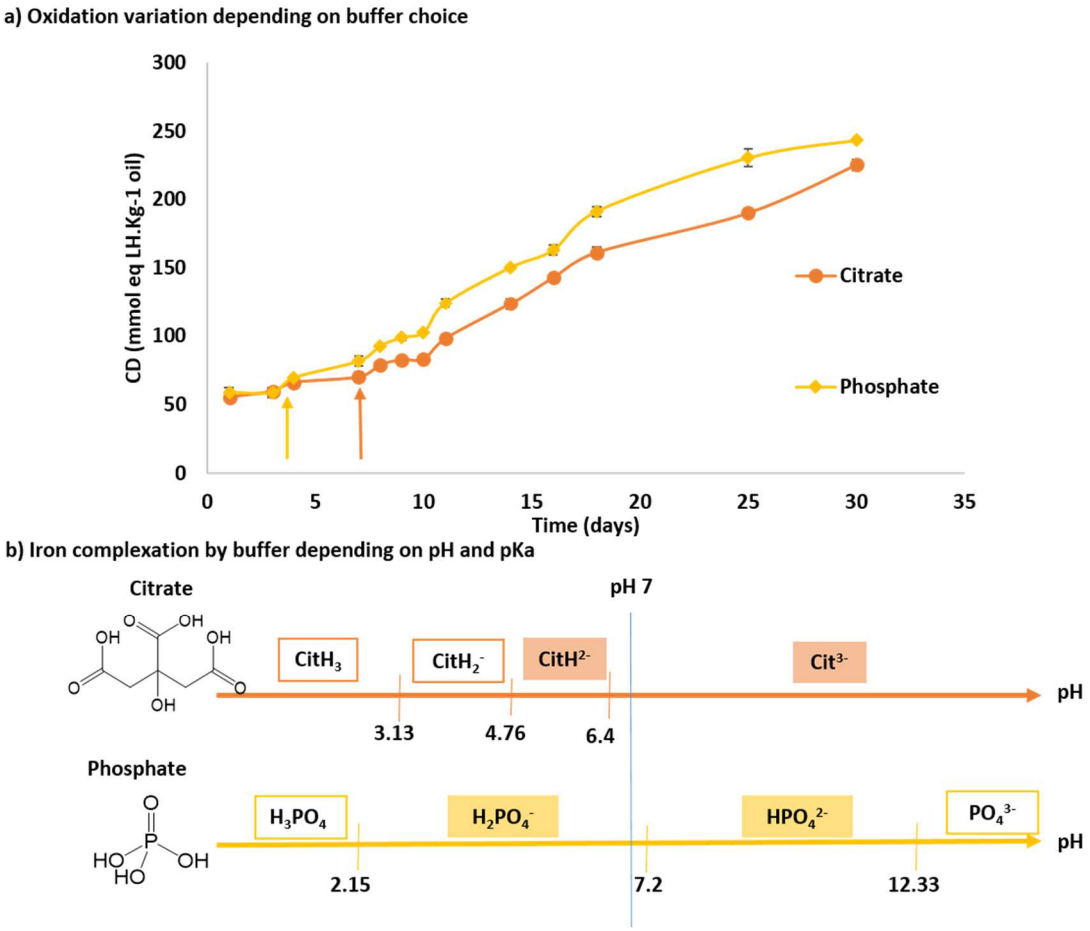

Figure 2. Buffer influence on iron-induced lipid oxidation: (a) Variations of CD value (mmol eq peroxide.Kg^{-1} oil) of emulsions (20% v/v oil) oxidized with 0.1 mM of iron and kept in dark at 30 °C. Different buffers (1 mM) were used: (●) citrate and (◊) phosphate. Data shown as means of three replicates and the error bars represent the standard deviation (sometimes laying within the points). Arrows indicate the induction times. (b) Distribution of buffer species depending on its pKa values. The pH of all the emulsions was set at 7. Species highlighted are theoretically the most abundant at pH 7

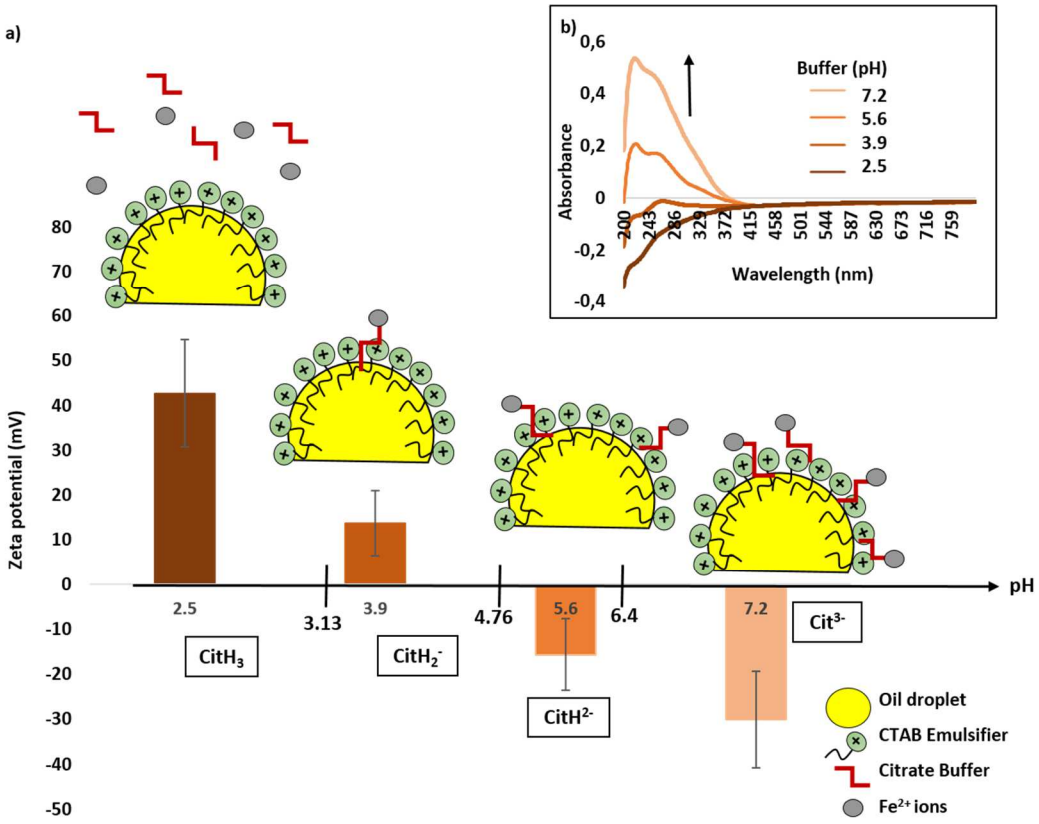

Figure 3. Impact of the pH level: (a) Variations of zeta potential (mV) of oil-in-water emulsions prepared using the citrate buffer (1 mM) at different pH level (2.5, 3.9, 5.6 and 7.2) and a simplified proposed design for the oil-water interface at different pH (iron ions complexation by citrate buffer and transfer to the interface). Iron was added to a final concentration of 0.1 mM. Values represent means of 6 repetitions (3 measurements on two different sets). Error bars represent standard deviations; (b) Differential UV spectra of iron (0.1 mM) and citrate (1 mM) solutions, these solutions were similar but at different pH levels, the peak of iron-citrate complex increases when the pH increased

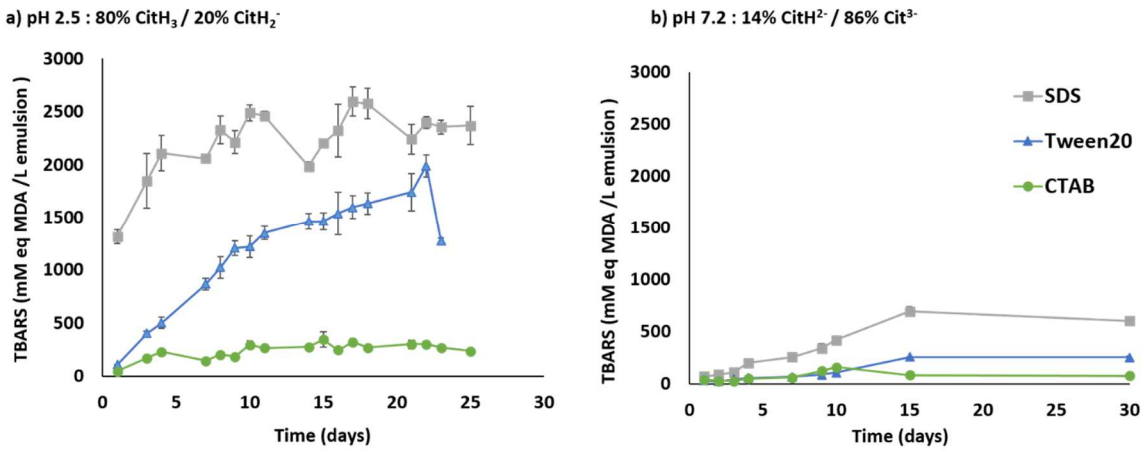

29

30 Figure 4. Variations in the oxidation level of oil-in-water emulsion (20 %v/v tuna oil) as
31 evaluated by the TBArs value (mM of eq MDA.L^{-1} emulsion) at pH 2.5 (a) and pH 7.2 (b). All
32 emulsions were prepared with citrate buffer (1 mM) with added iron (II) (0.1 mM), and kept in
33 dark at 30 °C. Three different emulsifiers were used: (●) $CTAB^{+}$ (cetyltrimethylammonium
34 bromide, positively charged), (▲) $Tween^{0}$ (Tween20, neutral) and (■) SDS^{-} (sodium
35 dodecylsulfate, negatively charged). Data represent means of three repetitions and error bars
36 are standard deviations

1 Table 1. Characterization of tuna oil used in this study: fatty acids composition, tocopherol

2 and iron contents

Fatty acids	Mean % wt. 3
14:0	3.43 ± 0.31
15:0	0.87 ± 0.08
16:0	19.51 ± 0.53
17:0	1.17 ± 0.06
18:0	6.12 ± 0.17
19:0	0.25 ± 0.04
Total SFA	**31.35**
16:1 (n-7)	5.22 ± 0.38
17:1	0.66 ± 0.04
18:1 (n-9)	18.82 ± 0.68
20:1	1.82 ± 0.15
22:1	0.28 ± 0.04
Total MUFA	**26.79**
16:2	1.32 ± 0.18
18:2 (n-6) (LA)	1.92 ± 0.08
20:4 (n-6)	1.84 ± 0.43
20:5 (n-3)(EPA)	8.92 ± 0.91
22:5	1.92 ± 0.07
22:6 (n-3) (DHA)	25.26 ± 0.63
Total PUFA	**41.17**
DHA/EPA	**2.83**
Total n-3	**34.18**
Total n-6	**3.76**
Iron ($mg.Kg^{-1}$ $_{oil}$)	**0.71 ± 0.35**
α-tocopherol ($mg.Kg^{-1}$ $_{oil}$)	**1282 ± 209**